

## Spin-current rectification in molecular wires

Hugh Dalglish and George Kirczenow

Department of Physics, Simon Fraser University, Burnaby, British Columbia, Canada V5A 1S6

(Received 25 March 2006; revised manuscript received 23 May 2006; published 29 June 2006)

We propose that spin current rectification in molecular junctions can take two different forms consistent with thermodynamic considerations: A *weak* form in which the spin current reverses direction when the bias applied to the junction is reversed and a *strong* form in which the direction of the spin current is unchanged upon reversal of the bias. We present calculations of spin-dependent transport in several molecular junctions bridging ferromagnetic (Fe or Ni) and nonmagnetic (Au or Pd) contacts and identify specific systems that should exhibit spin current rectification of each type in appropriate ranges of the applied bias voltage. Our results indicate that molecular junctions displaying both spin-current and charge-current rectification should be possible, and may find practical application in nanoscale devices that combine logic and memory functions.

DOI: [10.1103/PhysRevB.73.235436](https://doi.org/10.1103/PhysRevB.73.235436)

PACS number(s): 73.40.Ei, 85.65.+h, 85.75.-d, 73.63.-b

### I. INTRODUCTION

Rectification of electric current in molecular electronic devices [ $I(-V) \neq -I(V)$ ] is generally attributed to spatial asymmetries that manifest as asymmetries in the electronic characteristics of the device. Positive or negative bias voltages applied across the two terminals of the asymmetric device give rise to electronic eigenstates that contribute differently to the current causing the asymmetry under bias inversion. Such spatial asymmetry, and therefore rectification, may result from the use of spatially asymmetric molecules, different materials for source and drain electrodes, asymmetric molecule-lead binding, or a combination of all three.<sup>1-10</sup>

Utilization of *magnetic* materials as source and/or drain electrodes opens up the possibility of spin injection into a nonmagnetic or magnetic electrode through a molecular bridge.<sup>11</sup> As with the electronic (charge) current, spatial asymmetry in such a device may result in the net *spin* current,  $I_S$ , being asymmetric under bias inversion. However, although there have been several theoretical studies of spin transport through molecular junctions<sup>11-16</sup> the possibility of spin-current rectification in such systems has not been explored. We take up this topic in the present paper.

While thermodynamics requires the electronic current to *reverse* direction when the bias is reversed, there is no such requirement for the spin-current. Therefore we propose that spin-current rectification of two kinds should be possible in principle in spatially asymmetric systems:

(1) *Weak* spin-current rectification where the direction of the spin current reverses and the magnitude of the spin current changes when the applied bias is reversed; this is the spin analog of charge-current rectification.

(2) *Strong* spin-current rectification where the direction of the spin-current remains *unchanged* when the applied bias is reversed. This effect has no charge-current analog.

In the remainder of this paper we explore the possibility of spin-current rectification occurring in specific asymmetric molecular junctions theoretically and predict that both *weak* and *strong* spin-current rectification should be realized in practice, depending on the details of the system and the magnitude of the applied bias voltage.

As with charge-current rectification, spin-current rectifi-

cation is a *nonlinear* transport phenomenon; at infinitesimal bias (in the linear response regime) no rectification is possible. *Weak* spin-current rectification becomes possible in asymmetric magnetic junctions as the system exits the linear regime with increasing bias, and we predict *strong* spin-current rectification to be attainable in some systems at still higher bias. Therefore the above predictions regarding the nature of spin-current rectification are relevant to asymmetric junctions that can sustain a significant bias, such as molecular and nanoscale atomic junctions and metal/insulator/metal thin film systems.<sup>17</sup>

Because weak spin rectification is closely tied to current rectification, our findings demonstrate that it should be possible to design molecular electronic devices that *simultaneously* function as current rectifiers and spin rectifiers, thereby providing such molecular devices with dual functionality based on the transport of both charge and spin. Such functionality may ultimately allow both logic and memory to be implemented with a single device, and the design of such a device based on molecules may allow for its construction using the smallest possible circuit elements.

This paper is organized as follows: In Sec. II we describe our model of the geometries and electronic structures of the molecular junctions, and also briefly summarize the formalism used in our transport calculations. In Sec. III A our formalism and analysis are applied to asymmetric junctions where a single octane-thiolate (OT) or octane-dithiolate (OdT) molecule bridges the gap between Au or Pd and ferromagnetic Fe electrodes. We predict these molecular junctions to function as a current and spin-current rectifiers, and to exhibit both *weak* and *strong* spin-current rectification, depending on the value of the applied bias. In Sec. III B we consider a junction in which an OT molecule bridges Au and Ni electrodes. We predict less pronounced charge and spin-current rectification effects in this system than in the corresponding one with an Fe contact. Our conclusions are summarized in Sec. IV. Finally, in the Appendix we briefly discuss charging and electronic correlation effects within the molecule in relation to transport in these systems.

### II. THEORY

In our calculations the molecular system is partitioned into semi-infinite ideal source and drain leads and an ex-

tended molecular junction consisting of the molecule and clusters of nearby metal atoms. Each metallic cluster of the extended molecule is built from  $5 \times 5, 4 \times 4, 3 \times 3, 2 \times 2$  (100)-oriented layers (54 atoms total) of atoms in the bulk geometry of the metal. The molecular and molecule-metal binding geometries are estimated with *ab initio* relaxations.<sup>18</sup>

The electronic structure of the metal clusters is described by a tight-binding Hamiltonian and nonorthogonal  $s, p, d$  basis. The tight-binding parameters are based on fits to *ab initio* band structures of the metal crystals;<sup>19</sup> spin-up and spin-down electrons are treated independently for ferromagnetic materials in Ref. 19. Parameters taken from Ref. 19 have been successfully employed to study transport in magnetic nanocontacts,<sup>20,21</sup> and ferromagnetic Ni<sup>11</sup> and Fe<sup>16</sup> molecular junctions. When used to describe Fe nanoclusters,<sup>21</sup> this model yielded magnetic moments for surface and interior atoms in very close agreement with *ab initio* calculations.<sup>22</sup> Similarly, for larger Fe structures with surfaces,<sup>21</sup> this model yields spin-resolved surface densities of states and enhanced surface magnetic moments similar to those of *ab initio* surface calculations.<sup>23</sup> Thus our model incorporates *both* the bulk and surface electronic properties of the metals which together influence the spin-dependent transport through a nanoscale junction of bulk metal leads bridged with molecules.

The molecular electronic parameters as well as the electronic parameters describing the molecular coupling to the metal electrodes are described by a tight-binding formalism based on extended-Hückel (EH) theory.<sup>24</sup> This approach has been used successfully to explain the experimental current-voltage characteristics of molecular nanowires connecting Au electrodes.<sup>25-27</sup> The EH parameters are based on atomic ionization energies while the electronic parameters from Ref. 19 describing the metal clusters are defined up to an arbitrary additive constant. We adjust this constant to align the Fermi energy of the contacts relative to the highest occupied molecular orbital (HOMO) of the molecule, according to the difference between the work function of the metal and the HOMO energy of the isolated molecule obtained from density functional theory,<sup>18</sup> a method that has been used previously to align the Fermi energy of gold<sup>28</sup> and iron<sup>16</sup> relative to molecular HOMO levels.

When different metals are used for the two electrodes of the molecular device their differing work functions give rise to electrostatic fields between the electrodes even if no bias is applied across the device. This *contact potential*-related field<sup>29</sup> is included approximately in our model. It is treated in a similar way to that created by application of bias (discussed below), but with the molecular atomic site energies being shifted according to a linear potential profile.

Our transport calculations are based on Landauer theory<sup>30</sup> and Lippmann-Schwinger and Green's function techniques. Landauer theory relates the current to the multichannel probability  $T$  for an electron to scatter from the source electrode to the drain via the junction, according to

$$I(V) = \frac{e}{h} \int dE T(E, V) [f(E, \mu_S) - f(E, \mu_D)], \quad (1)$$

where  $E$  is the energy of the electron,  $f(E, \mu)$  is the equilibrium Fermi distribution and  $\mu_{S,D} = E_F \pm eV/2$  are the electro-

chemical potentials of the source ( $S$ ) and drain ( $D$ ) electrodes in terms of the common Fermi energy,  $E_F$ . As the spin-resolved transmission resonances that are responsible for transport at moderate bias in the molecular wire systems considered here differ in energy by over 1 eV, moderate temperatures (such as room temperature) are expected to have a relatively minor impact on our qualitative predictions. Thus only zero temperature is considered here.

Spin-flip processes are not considered, consistent with weak spin-orbit interaction in molecules and the high degree of spin polarization retained in observations of spin-dependent transport in molecular junctions;<sup>31-33</sup> for ferromagnetic electrodes the parameters describing spin-up and spin-down electrons are separately applied and the transmissions and currents are calculated independently for spin-up [ $I_{\uparrow}(V)$ ] and spin-down [ $I_{\downarrow}(V)$ ] electrons. The total current through the molecular device is given by the sum of the currents for the separate spin channels  $I(V) = I_{\uparrow}(V) + I_{\downarrow}(V)$  while the net spin (angular momentum) current is given by

$$I_S(V) = \frac{\hbar}{2e} [I_{\downarrow}(V) - I_{\uparrow}(V)]. \quad (2)$$

A detailed discussion of our theoretical formalism has been presented elsewhere.<sup>16,21</sup>

Since rectification is attainable only under the application of significant bias, finite bias effects must be included explicitly in our model. The potential profile of a molecular junction arising from the bias voltage applied between the two electrodes is a complex nonequilibrium many-body property, and therefore is difficult to calculate from first principles. However, appropriate heuristic models for the profile can yield accurate results for the current: It has been shown<sup>34</sup> by comparison with the results of *ab initio* calculations (that include the electronic correlation energies of molecular wires and their electric field dependence in a mean field approximation) that the effects of screening and charging on transport in simple molecular wires can be modeled accurately by employing appropriate phenomenological potential profiles between the metal contacts. We adopt this approach here,<sup>35</sup> and note that our qualitative predictions are not sensitive to the precise details of the model profiles that we use. Most of the molecular bridges considered in this work are monothiolates, and for these systems a substantial spatial gap is predicted at the interface between the metal contact and the nonthiolated molecular end. In the numerical results presented here for these systems we assume for simplicity that one-half of the applied bias drops at this interface and one-half drops across the molecule.<sup>36</sup> Our predictions regarding the *strong* and *weak* spin-current rectification regimes do not change qualitatively if other model potential profiles are adopted.

### III. RESULTS

#### A. Au/OT/Fe, Au/OdT/Fe, and Pd/OT/Fe

The extended molecule for the Au/OT/Fe molecular junction is shown in the inset of Fig. 1(a). The sulfur atom is estimated to sit 2 Å above the fourfold FCC Au hollow site,

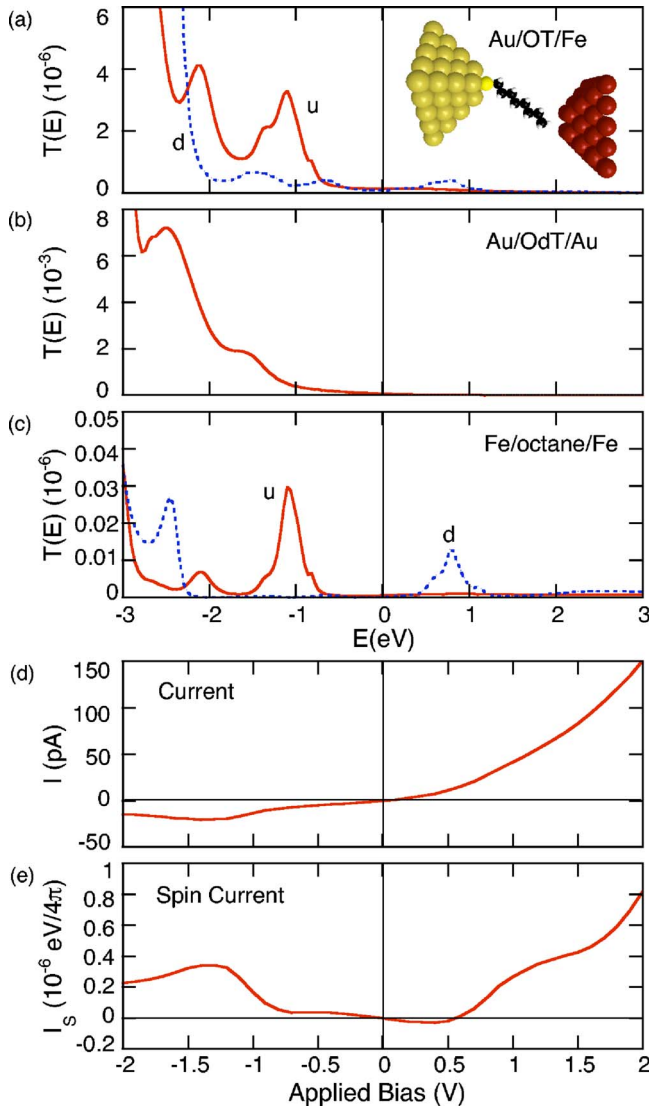


FIG. 1. (Color online) (a) Transmission probabilities vs energy at zero bias for spin-up ( $u$ ) and spin-down ( $d$ ) electrons for the Au/OT/Fe molecular junction displayed in the inset. Fermi energy  $= 0$  eV. (b) Transmission probability for an Au/OdT/Au junction. (c) Transmission probabilities for an Fe/octane/Fe junction. (d) Calculated current vs voltage for the Au/OT/Fe junction in (a). (e) Calculated net spin-down current given by Eq. (2) vs voltage.

while the BCC Fe electrode surface is estimated to be  $4.1 \text{ \AA}$  from the molecular carbon atom.<sup>18</sup> Such molecular junction geometries may be realized with STM or break junction systems where the Fe-C distance may vary. However, while the magnitudes of the currents depend exponentially on the Fe-C separation, the qualitative transmission features and ratios of currents are insensitive to the separation for a wide range of values. Our qualitative predictions are also not overly sensitive to the metal-S distance.

The calculated transmission probabilities at zero bias for spin-up ( $u$ ) and spin-down ( $d$ ) electrons are displayed in Fig. 1(a) for the Au/OT/Fe junction; the common Fermi level of the metal contacts is at 0 eV. The mechanisms that give rise to the resonant transmission features that are visible near  $-1$  eV and  $0.8$  eV at zero bias in Fig. 1(a) control both the

charge current  $I$  [Fig. 1(d)] and the spin current  $I_S$  [Fig. 1(e)] at moderate bias. These mechanisms involve interactions of the molecule with both metal interfaces; to understand them it is helpful to examine the roles of the two different metal-molecule interfaces separately. We do this by considering a pair of closely related *symmetric* molecular wire systems, Au/octane-dithiolate/Au and Fe/octane/Fe. In the former system both metal-molecule interfaces are similar to the Au/molecule interface of Au/OT/Fe while in the latter both are similar to the Fe/molecule interface of Au/OT/Fe.<sup>37</sup> The calculated zero bias transmission probabilities for these two symmetric systems are plotted in Fig. 1(b) and Fig. 1(c), respectively; for the Fe/octane/Fe system parallel magnetization of the two Fe electrodes is assumed and both the spin-up and spin-down electron transmission probabilities are shown. Since transmission features due to the interaction of the molecule with the source and drain interfaces are degenerate at zero bias for symmetric junctions, the analysis of the transmission probabilities in Figs. 1(a)–1(c) are more straightforward than of those in Fig. 1(a):

For the symmetric Au/OdT/Au junction, the weak transmission resonance near  $-1.5$  eV in Fig. 1(b) is due to resonant conduction through the molecular HOMO. The conduction is weak because the HOMO is localized mainly at and near the sulfur atoms and decays rapidly along the molecule's carbon backbone. The transmission probability decreases towards the Fermi energy where it is due to off-resonant conduction via the tail of the HOMO resonance. The large transmission below the HOMO resonance is due to molecular conducting states lower in energy, including the HOMO-1. The lowest unoccupied molecular orbital (LUMO) is located above the plotted energy range due to the large molecular HOMO-LUMO gap (OdT and OT are insulators) and does not contribute significantly to the current for any of the results presented in this work. Due to the resonant conduction through the HOMO and its off-resonant transmission near the Fermi energy, the transmission probability for Au/OdT/Au is quite asymmetric about the Fermi energy ( $E_F = 0$  eV). Nevertheless, for a *spatially* symmetric junction,  $I(-V) = -I(V)$  and rectification is not possible. However, the asymmetry of  $T(E)$  about  $E_F$  for the Au/molecule contact can result in strong rectification when this contact forms part of an *asymmetric* molecular junction (as for Au/OT/Fe) and the total transmission at the second contact is symmetric about  $E_F$ .

Such is nearly the case for the Fe contact as is displayed in Fig. 1(c) [while the total transmission  $T(E) = T_{\uparrow}(E) + T_{\downarrow}(E)$  is asymmetric about the Fermi energy, with the magnitudes of the  $u$  and  $d$  transmission peaks differing by roughly a factor of 2, it is much less so than  $T(E)$  in Fig. 1(b)]. As is the density of states for bulk Fe,<sup>19</sup> the features in the transmission in Fig. 1(c) are highly spin split: The transmission features near 1 eV below  $E_F$  for spin-up and 0.8 eV above  $E_F$  for spin-down in Fig. 1(c) are due to Fe metal states. They are present even in the *absence* of molecules [as reported in Fig. (6a) in Ref. 21 for vacuum tunneling between Fe nanocontacts]; since there is no strong hybridization between the octane molecule and either Fe contact, the main role of the octane is to effectively lower the

barrier for conduction in the Fe/octane/Fe junction. Because of this our qualitative predictions are insensitive to variations in the C-Fe distance: While variations affect the strength of the Fe metal state transmission resonances (and thus scale the magnitude of the current) the energy locations and *relative* strengths of these resonances are robust to such variations.

The origin and qualitative characteristics of the important features in the transmission of the asymmetric Au/OT/Fe molecular junction seen in Fig. 1(a) are now readily understood as manifestations of consecutive transmission of electrons through the Au/OT and OT/Fe interfaces: The prominent spin-up transmission feature in Fig. 1(a) around  $-1$  eV is due to the peak in the spin-up transmission between the Fe and the molecule in this energy range [Fig. 1(c)] coinciding with the molecular HOMO-mediated transmission at the Au/OT interface [Fig. 1(b)]. The much weaker spin-down transmission feature around  $0.8$  eV in Fig. 1(a) is due to the corresponding peak in the spin-down transmission between the Fe and the molecule [Fig. 1(c)] occurring in an energy range where there is no transmission resonance associated with the Au/OT interface. The similarly weak spin-down transmission around  $-1$  eV in Fig. 1(a) is due to weak spin-down transmission at the OT/Fe interface coinciding with the (broad) molecular HOMO-mediated transmission resonance associated with the Au/OT interface.

The total charge current,  $I(V) = I_{\uparrow}(V) + I_{\downarrow}(V)$ , displayed in Fig. 1(d) as a function of applied bias voltage  $V$  is calculated according to the Landauer expression, Eq. (1) from the bias-dependent transmission probability  $T(E, V)$ . The latter quantity differs from  $T(E, 0)$  that is plotted in Fig. 1(a) in that  $T(E, V)$  includes the effects of the bias voltage on the energies of the electronic states within the metal contacts as well as on the potential profile of the molecular junction as was discussed in Sec. II. However, the behavior of the current can still be understood qualitatively in terms of electron transmission through the two molecule-metal interfaces discussed above if their bias dependence is taken into consideration: With increasing positive bias (applied to the Fe electrode) the transmission features due to the molecular HOMO levels that are associated with the Au/molecule interface [Fig. 1(b)] move to higher energies relative to the transmission features due to the Fe/molecule interface [Fig. 1(c)]. This results in an overall enhancement of  $T(E, V)$  relative to  $T(E, 0)$  within the window of conduction between the electro-chemical potentials of the source and drain electrodes, defined by Eq. (1). By contrast, for negative applied bias the transmission features due to the Au/molecule interface [Fig. 1(b)] move to lower energies and remain *outside* the window of conduction, resulting in an overall weakening of  $T(E, V)$ . Thus the magnitude of the current  $I$  at positive bias is markedly larger than that at negative bias, so that the Au/OT/Fe molecular junction behaves as a charge-current rectifier as is evident in Fig. 1(d).<sup>38</sup>

The net spin current given by Eq. (2) is displayed in Fig. 1(e). As expected from general considerations (see Sec. I) there is a linear response regime at low bias (in this case for  $|V|$  below approximately  $0.4$  V) where there is no appreciable spin-current rectification, followed by (for  $|V|$  below

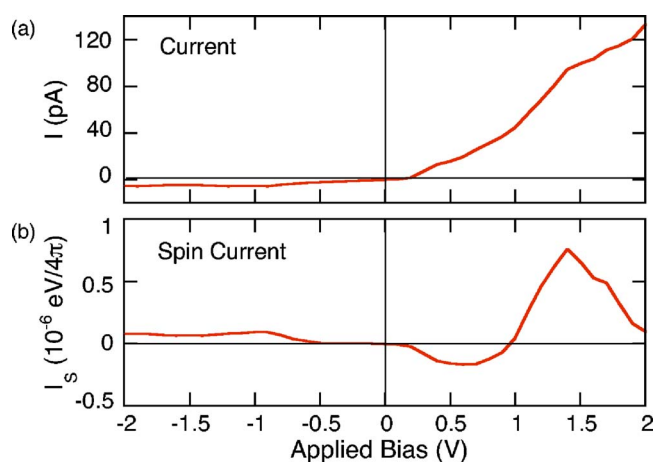


FIG. 2. (Color online) (a) Calculated current-voltage characteristic for the Pd/OT/Fe junction. (b) Net spin current [Eq. (2)] vs voltage.

approximately  $0.6$  V) the onset of appreciable nonlinearity with an associated *weak* spin-current rectification regime where  $I_S(V) \neq -I_S(-V)$  although  $I_S(V)$  and  $I_S(-V)$  have opposite signs. However at still larger bias our calculations predict a qualitative change in the nature of the spin-current rectification: The net spin current is positive for *both* directions of applied bias voltage over a substantial voltage range beginning near  $\pm 0.6$  V, i.e., *strong* spin-current rectification is predicted. This is due to the asymmetry about the Fe Fermi level of the spin-up and spin-down transmission resonances associated with the Fe/molecule interface that is evident also in Fig. 1(c). For positive bias applied on the Fe contact the transmission is dominated by the transport of spin-down electrons through the molecule from the Au into unoccupied states of the Fe contact that are predominantly spin down. For similarly large negative bias, the transport is dominated by spin-up electrons as the occupied states on the Fe contact are predominantly spin up. Therefore, for either direction of bias, the net spin-down electron flux is towards the Fe contact.

Our calculations for an Au/octane-*dithiolate*(OdT)/Fe molecular junction predict that this system should also function as a *strong* spin-current rectifier comparable to Au/OT/Fe. The mechanisms involved are however somewhat different for the two systems: Whereas the spin rectification in the Au/OT/Fe system arises from spin-split Fe metallic states at the unbonded Fe interface [as in Fig. 1(c)], *both* contacts are thiol-bonded for Au/OdT/Fe. In this case, the low bias transmission on the Fe contact is dominated by *interface states* at the sulfur-Fe interface [see Fig. 1(a) in Ref. 16] that are also spin-split and occur on opposite sides of the Fe Fermi energy.

Our calculations also predict similar spin rectification to that in Fig. 1(e) if the Au electrode is replaced with Pd.<sup>39</sup> Here, due to the strong hybridization that occurs between the molecular sulfur atom and the *d*-electronic states of the Pd contact, the moderate bias transmission on the Pd/molecule contact is dominated by interface states that develop within the HOMO-LUMO gap.<sup>10</sup> They are located near the HOMO (below the Fermi energy) and as a result the transmission at

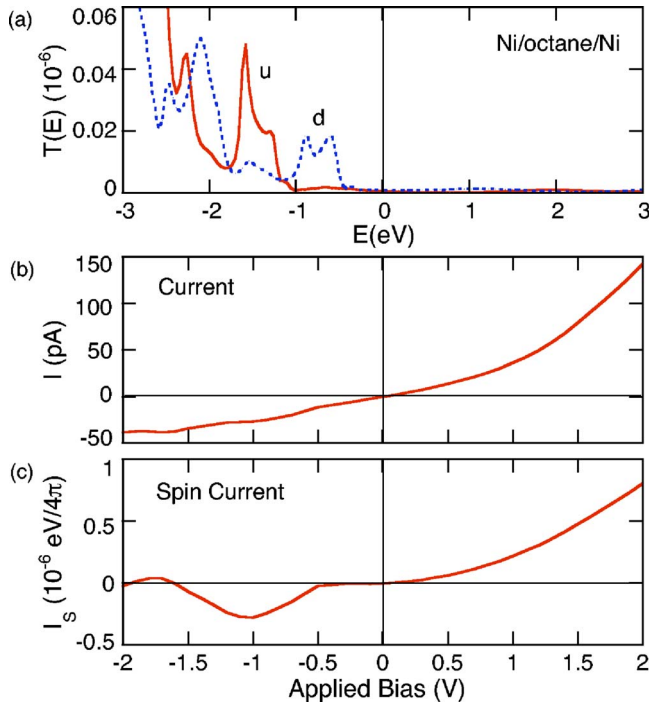


FIG. 3. (Color online) (a) Zero bias transmission probabilities for spin-up (u) and spin-down (d) electrons for a Ni/octane/Ni molecular junction. (b) Calculated current-voltage characteristic for the Au/OT/Ni junction. (c) Net spin current [Eq. (2)] vs voltage.

the Pd/molecule contact is even more asymmetric about the zero bias Fermi energy than the transmission due to the Au/molecule contact [Fig. 1(c)].

The calculated total current  $I$  for the Pd/OT/Fe molecular junction is displayed in Fig. 2(a). Due to the large transmission asymmetry at the Pd/molecule contact, the current exhibits stronger charge current rectification (the current is more asymmetric under inversion of bias) than that displayed in Fig. 1(d) for the Au/OT/Fe junction. Also, as is evident from the calculated spin current  $I_s$  plotted in Fig. 2(b), the Pd/OT/Fe junction possesses significant *weak* spin rectification beginning for  $|V|$  above 0.2 V and extending to applied biases of  $\pm 1$  V. Since the transmission at the molecule/Fe contact is unchanged, the *strong* spin-current rectification for  $|V|$  above 1 V in Fig. 2(b) is qualitatively similar to that in Fig. 1(e).

### B. Au/OT/Ni

Figure 3 shows the predicted transmissions and currents for an Au/OT/Ni molecular junction (the Ni-C separation is the same as the Fe-C separation considered in Sec. III A). In this case the transmission probabilities for Ni/octane/Ni displayed in Fig. 3(a) serve to clarify the nature of the transmission at the Ni/molecule interface; Fig. 1(b) relates to the Au/molecule interface for the Au/OT/Ni system as well.

Since the Ni/molecule transmission resonances are located below the Fermi energy for *both* spin-up ( $u$ ) and spin-down ( $d$ ) electrons in Fig. 3(a), in contrast to the Fe/molecule transmission resonances in Fig. 1(c), the current and spin-current rectification properties of Au/OT/Ni are pre-

dicted to be significantly different than for Au/OT/Fe and Pd/OT/Fe.

The total current  $I$  for Au/OT/Ni is displayed in Fig. 3(b). The asymmetry in the magnitude of the current between positive and negative bias voltage is not as strong in Fig. 3(b) as in Fig. 1(d) or 2(a). This is a result of the transmission resonances associated with the Ni contact being located below the Fermi energy for both spin configurations: As they are located similarly to the resonance for Au/OdT/Au in Fig. 1(b) (though they are smaller in magnitude), the effective asymmetry between the source and drain contacts is reduced relative to the molecule/Fe systems resulting also in a reduction of the strength of the charge current rectification. For the same reason, as is evident from Fig. 3(c), spin-current rectification is predicted to be a much less pronounced phenomenon in the Au/OT/Ni molecular junction than for either Au/OT/Fe or Pd/OT/Fe: *Weak* spin rectification is predicted to extend over a wider bias range for the Au/OT/Ni molecular junction than for the Fe junctions, and *strong* spin rectification is predicted to be largely or completely suppressed in the Au/OT/Ni junction; while slightly positive,  $I_s$  is very close to zero around  $-1.75$  V in Fig. 3(c).

## IV. CONCLUSIONS

In summary, we have proposed that spin-current rectification in molecular junctions can take two different forms consistent with thermodynamic considerations: A *weak* form in which the spin-current reverses direction when the bias applied to the junction is reversed and a *strong* form in which the direction of the spin current is unchanged upon reversal of the bias. We have presented calculations of spin-dependent transport in several molecular junctions in which one metal contact is nonmagnetic and the other consists of Fe or Ni. We have predicted both types of spin-current rectification to occur (depending on the bias voltage) in the junctions with Fe, and the weak form to occur for Ni contacts. Our results indicate that molecular junctions displaying both spin-current and charge-current rectification should be possible, and may find practical application as nanoscale devices that combine<sup>40</sup> logic<sup>41,42</sup> and memory<sup>43</sup> functions. Experimental observation and further theoretical studies of the phenomena that we have predicted here would be of interest.

## ACKNOWLEDGMENTS

This work was supported by NSERC and the Canadian Institute for Advanced Research.

## APPENDIX: DISCUSSION OF CHARGING AND CORRELATION EFFECTS

Since we are considering insulating alkane-thiolate molecules that behave primarily as potential barriers that contain no electronic trapping centers, neither charging of the molecules in response to applied bias nor any associated strong electronic correlation effects originating within the molecules are expected to play an important role in transport through these systems. In our calculations, the HOMO of octane-thiolate comes close to the window between the

chemical potentials of the source and drain at the highest bias voltages we consider (2V), for positive bias applied on the iron contact. However, since the HOMO is filled, and the molecule is strongly coupled to the source contact, the HOMO is not expected to charge significantly. The HOMO does not come close to the current window under reverse bias for the moderate bias results presented here. The metallic states that dominate the current in the moderate bias regime are located mainly within the metal contacts and are well separated in energy from the Fermi levels of their respective leads. They are strongly coupled to their respective electrodes, whereas the calculated electron transmission

probabilities via electrode to electrode are very low,  $<10^{-5}$ . Thus these states are always close to being in equilibrium with their respective electrodes and are therefore not expected to charge (i.e., change their electron occupations) appreciably in response to the application of bias. Furthermore, because of the large HOMO-LUMO gap of the alkane-thiols that we consider, the molecular LUMO levels are located at energies that are too high for them to become charged at any reasonable bias voltages. Because charging of the alkane-thiolate molecule in response to applied bias is not expected to be important, we expect mean field theory to be applicable to transport in these systems.

- <sup>1</sup>A. Aviram and M. A. Ratner, Chem. Phys. Lett. **29**, 277 (1974).  
<sup>2</sup>V. Mujica, M. Kemp, A. Roitberg, and M. Ratner, J. Chem. Phys. **104**, 7296 (1996); V. Mujica, M. A. Ratner, and A. Nitzan, Chem. Phys. **281**, 147 (2002).  
<sup>3</sup>A. Dhirani, P.-H. Lin, P. Guyot-Sionnest, R. W. Zehner, and L. R. Sita, J. Chem. Phys. **106**, 5249 (1997).  
<sup>4</sup>C. Zhou, M. R. Deshpande, M. A. Reed, L. Jones II, and J. M. Tour, Appl. Phys. Lett. **71**, 611 (1997).  
<sup>5</sup>C. Krzeminski, C. Delerue, G. Allan, D. Vuillaume, and R. M. Metzger, Phys. Rev. B **64**, 085405 (2001).  
<sup>6</sup>P. E. Kornilovitch, A. M. Bratkovsky, and R. S. Williams, Phys. Rev. B **66**, 165436 (2002); B. Larade and A. M. Bratkovsky, *ibid.* **68**, 235305 (2003); S.-C. Chang, Z. Li, C. N. Lau, B. Larade, and R. S. Williams, Appl. Phys. Lett. **83**, 3198 (2003).  
<sup>7</sup>F. Zahid, A. W. Ghosh, M. Paulsson, E. Polizzi, and S. Datta, Phys. Rev. B **70**, 245317 (2004).  
<sup>8</sup>R. M. Metzger, Macromol. Symp. **212**, 63 (2004).  
<sup>9</sup>G. Ho, J. R. Heath, M. Kondratenko, D. F. Perepichka, K. Arsenault, M. Pérolet, and M. R. Bryce, Chem.-Eur. J. **11**, 2914 (2005).  
<sup>10</sup>H. Dalglish and G. Kirczenow, Phys. Rev. B **73**, 245431 (2006).  
<sup>11</sup>E. G. Emberly and G. Kirczenow, Chem. Phys. **281**, 311 (2002).  
<sup>12</sup>M. Zwolak and M. Di Ventra, Appl. Phys. Lett. **81**, 925 (2002).  
<sup>13</sup>R. Pati, L. Senapati, P. M. Ajayan, and S. K. Nayak, Phys. Rev. B **68**, 100407(R) (2003).  
<sup>14</sup>W. I. Babiacyk and B. R. Bulka, J. Phys.: Condens. Matter **16**, 4001 (2004).  
<sup>15</sup>A. R. Rocha, V. M. García-Suárez, S. W. Bailey, C. J. Lambert, J. Ferrer, and S. Sanvito, Nat. Mater. **4**, 335 (2005).  
<sup>16</sup>H. Dalglish and G. Kirczenow, Phys. Rev. B **72**, 184407 (2005).  
<sup>17</sup>Experimental work has demonstrated a variety of molecular wires to support applied bias voltages in excess of 1 Volt without breaking down; see, for example, M. A. Reed, C. Zhou, C. J. Muller, T. P. Burgin, and J. M. Tour, Science **278**, 252 (1997); X. Li, J. He, J. Hihath, B. Xu, S. M. Lindsay, and N. Tao, J. Am. Chem. Soc. **128**, 2135 (2006).  
<sup>18</sup>The Gaussian 03 package (Rev. B.05) was used with the B3PW91 density functional and the Lanl2DZ basis set.  
<sup>19</sup>D. A. Papaconstantopoulos, *Handbook of the Band Structure of Elemental Solids* (Plenum, New York, 1986).  
<sup>20</sup>J. Velev and W. H. Butler, Phys. Rev. B **69**, 094425 (2004).  
<sup>21</sup>H. Dalglish and G. Kirczenow, Phys. Rev. B **72**, 155429 (2005).  
<sup>22</sup>O. Šipr, M. Košuth, and H. Ebert, Phys. Rev. B **70**, 174423 (2004).  
<sup>23</sup>S. Ohnishi, A. J. Freeman, and M. Weinert, Phys. Rev. B **28**, 6741 (1983).  
<sup>24</sup>S. P. McGlynn, L. G. Vanquickenborne, M. Kinoshita, and D. G. Carrol, *Introduction to Applied Quantum Chemistry* (Holt, Rinehart and Winston, New York, 1972), Chaps. 2–4.  
<sup>25</sup>S. Datta, W. Tian, S. Hong, R. Reifenberger, J. I. Henderson, and C. P. Kubiak, Phys. Rev. Lett. **79**, 2530 (1997).  
<sup>26</sup>E. G. Emberly and G. Kirczenow, Phys. Rev. Lett. **87**, 269701 (2001); Phys. Rev. B **64**, 235412 (2001).  
<sup>27</sup>J. G. Kushmerick, D. B. Holt, J. C. Yang, J. Naciri, M. H. Moore, and R. Shashidhar, Phys. Rev. Lett. **89**, 086802 (2002).  
<sup>28</sup>P. A. Derosa and J. M. Seminario, J. Phys. Chem. B **105**, 471 (2001).  
<sup>29</sup>R. E. Peierls *Quantum Theory of Solids* (Oxford University Press, London, 1956), Ch. 4.7.  
<sup>30</sup>For a review see S. Datta, *Electronic Transport in Mesoscopic Systems* (Cambridge University Press, Cambridge, 1995).  
<sup>31</sup>V. Dediu, M. Murgia, F. C. Matocotta, C. Taliani, and S. Barbanera, Solid State Commun. **122**, 181 (2002).  
<sup>32</sup>Z. H. Xiong, D. Wu, Z. V. Vardeny, and J. Shi, Nature (London) **427**, 821 (2004).  
<sup>33</sup>J. R. Petta, S. K. Slater, and D. C. Ralph, Phys. Rev. Lett. **93**, 136601 (2004).  
<sup>34</sup>S.-H. Ke, H. U. Baranger, and W. Yang, Phys. Rev. B **70**, 085410 (2004).  
<sup>35</sup>As the tight-binding basis is nonorthogonal, the effect of the electrostatic potential is included approximately in the form  $H_{ij} = H_{ij}^0 - eS_{ij}(\phi_i + \phi_j)/2$  where  $H_{ij}^0$  is the tight-binding Hamiltonian matrix at zero bias,  $S_{ij}$  is the overlap matrix and  $\phi_i$  is the electrostatic potential  $\phi$  at the site occupied by atomic orbital  $i$ . Thus in the present model the presence of electrostatic fields influences both diagonal and off-diagonal Hamiltonian matrix elements, including the molecule-electrode coupling. See Ref. 21 for further details.  
<sup>36</sup>Approximating the molecular wire system as a parallel-plate capacitor with plates separated by a heterogeneous junction formed from two materials with different dielectric constants (a molecular film with a dielectric constant of 2.5–3 and air) yields a potential profile where approximately 1–1.5 times as much bias drops over the molecule as over the vacuum gap.  
<sup>37</sup>The geometries of the symmetric junctions are obtained by geometrically mirroring the asymmetric Au/OT/Fe junction to the

left and to the right without further geometry relaxations. The Fermi energy alignment of the contacts is the same in all three model systems, using that of the Au/OT/Fe junction as the reference.

<sup>38</sup>In our figures we employ the standard sign convention for the electric current, namely, that a positive conventional current flows from the positively biased electrode to the negative one.

<sup>39</sup>The Pd-S binding distance is estimated to be 1.74 Å (Ref. 18).

<sup>40</sup>Two-terminal logic has been shown possible with molecular rectifying devices (Refs. 41 and 42). Controllable spin injection and

detection are required for memory devices that are based on electron spin (Ref. 43). Thus devices combining charge and spin current rectifying properties could in principle combine logic and memory functions.

<sup>41</sup>J. C. Ellenbogen and J. C. Love, Proc. IEEE **88**, 386 (2000).

<sup>42</sup>R. Stadler, S. Ami, M. Forshaw, and C. Joachim, Nanotechnology **14**, 722 (2003).

<sup>43</sup>S. A. Wolf, D. D. Awschalom, R. A. Buhrman, J. M. Daughton, S. von Molnár, M. L. Roukes, A. Y. Chtchelkanova, and D. M. Treger, Science **294**, 1488 (2001).